Synthesis of ZnO Nanostructures Using Sublimation–Condensation and Sol-Gel Methods: Evaluation of the Photocatalytic Degradation Activity of Industrial Dye

S. Harouni, N. Bouanimba* and N. Boulares

Laboratoire de Physique-chimie des semiconducteurs (LPCS), Département de Physique,

Faculté des Sciences Exactes, Université des Frères Mentouri Constantine, Algeria

ZnO nanostructures were prepared by sublimation–condensation (ZnO-SPVD) technique and sol-gel method (ZnO-SG). The produced materials were used in a photocatalytic degradation of a pollutant (gentian violet) at different operational conditions. The materials were characterized by X-ray diffraction (XRD) and Raman spectra techniques (RS). The obtained results indicated that the photocatalytic activity was correlated to the particle sizes of catalysts. The catalyst prepared by the physical method (ZnO-SPVD) exhibited a higher photoactivity to degrade GV dye than the catalyst prepared by the chemical method (ZnO-SG). In the presence of each of ZnO-SPVD or ZnO-SG, the experiments were carried out to investigate the factors that influence the photocatalytic degradation of GV, such as the adsorption amount, pH of dye solution, electron acceptors (H_2O_2), and presence of inorganic species commonly present in real wastewaters (HCO_3^-). The experimental results showed that adsorption on the surface of both samples was an important parameter controlling the photocatalytic activity. For both catalysts, the degradation rate in alkaline medium was higher than that in natural and acidic one. The presence of the H_2O_2 and HCO_3^- ions increased the effectiveness of the photodegradation.

1. Introduction

Zinc oxide is a very important material in some technological applications. It is commonly found in nature and can also be easily synthesized in the laboratory. It is widely used in catalysis, sensors, ceramics, and optoelectronic devices, due to its excellent optical, peizoelectrical, and magnetic properties [1, 2].

In recent years, the photocatalytic properties of ZnO were also extensively studied [3–6]. Owing to the rapid photoresponse and good photoelectric conversion properties, ZnO exhibits high photocatalytic efficiencies on decomposing organic pollutants in water. Additionally, unlike other semiconductors, ZnO is non-toxic, low cost, and suitable to work using sunlight as energy source, which make it an ideal candidate for practical applications on environmental treatments.

Many methods for the production of ZnO nanostructures have been described in the literature such as chemical or physical vapor deposition (CVD or PVD) [7, 8], sol–gel (SG) [9], hydrothermal [10], and precipitation methods [11], resulting in ZnO nanoparticles with a nanometric size.

In recent years advanced oxidation processes (AOPs) have been developed to meet the increasing need of an effective wastewater treatment. Heterogeneous photocatalysis, one of the AOPs, is a cost-effective treatment method for the removal of toxic pollutants from wastewater sowing to its ability to convert these pollutants into CO_2, H_2O, and mineral acids [12–14]. Synthetic dyes constitute one of the larger groups of pollutants in wastewater released from textile, leather tanning, paper production, plastics, and other industries. These dyes have a big impact on the environment because of their potential carcinogenic properties [15, 16].

In the photocatalytic process, semiconductor particles are irradiated with light energy equal to or greater than its band gap. It results in the formation of electron-hole pair. Electron (e^-) is present in conduction band, whereas hole (h^+) is present in the valence band. The detailed mechanism of the photocatalytic process has been discussed extensively in the literature [12–14].

In this paper, highly crystalline ZnO nanoparticles were synthesized by sublimation–condensation technique (ZnO-SPVD) and sol-gel method (ZnO-SG), and characterized by X-ray diffraction (XRD) and Raman spectra techniques (RS).

The study of the efficiency of the two series of zinc oxide samples was carried by the investigation of the photocatalytic activity by performing the decomposition of Gentian violet (GV) dye, a cationic triphenylmethane dye under UV illumination over each of the two synthesized catalysts.

———————

*corresponding author; e-mail: nourbouanimba@gmail.com

The investigated dye (Gentian violet) is extensively used in the textile, paper, and many industries. Gentian violet is hazardous compound and suspected to be toxic and carcinogenic for humans and animals [17, 18]. The efficiency of the GV photocatalytic degradation reaction was studied under different experimental conditions, the influence of several experimental parameters, such as the adsorption of dye onto ZnO surface, the initial dye concentration, the initial pH, the addition of HCO_3^- ion and the addition of hydrogen peroxide, upon the GV degradation rate constant was also investigated.

2. Materials and experimental methods

2.1. Reagents and chemicals

Gentian violet (GV, Biochem chemopharma, C.I: 42.555, molecular formula: $C_{25}H_{30}N_3Cl$, molecular weight $= 407.979$ g mol L^{-1}). The structure of GV is presented in Fig. 1. H_2SO_4 (98%, Merck) and NaOH (Carlo Erba) for pH adjustments. NaCl and $HaHCO_3$ (Prolabo), H_2O_2 (Labosi). All solutions were prepared with deionized ultrapure water from a Milli pure water (Milli-Q purification unit).
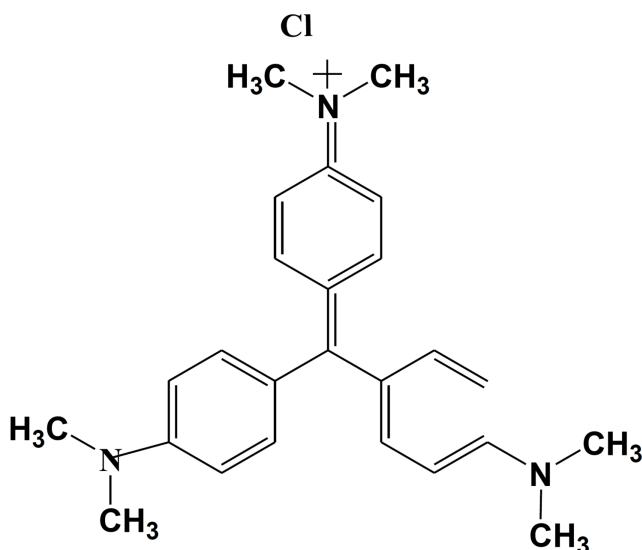

Fig. 1. Molecular structure of Gentian Violet (GV).

Sol-gel method: Nanoparticles of Zinc oxide were prepared by the sol-gel (citrate route) method using zinc acetate, $ZnC_4H_6O_4$ (Panreac), as the starting materials. Citric acid $C_6H_8O_7 \cdot H_2O$ (Panreac) was used as a complexing agent.

The sublimation–condensation technique: Nanoparticles of Zinc oxide were prepared by the sublimation–condensation under 660 Torr air pressure, in a solar reactor placed at the focus of a parabolic concentrator. The nanopowders were deposited on the spherical surface of a glass balloon [19].

2.2. Characterization of catalysts

2.2.1. Xray diffractometry (XRD):

To determine the phase composition and to estimate the mean crystallite size, powder X-ray diffraction (XRD) patterns were recorded for synthesized samples using PANalytical X'Pert Pro Philips X-ray diffractometer with CuK_α radiation, ($\lambda_{Cu} = 1.5418$ Å) and the accelerating voltage and current were 40 kV and 40 mA, respectively.

The XRD spectra of the obtained nanoparticles are shown in Fig. 2. The peaks appearing at 2θ range of $31°C$, $34°C$, $36°C$, $47°C$, $56°C$, and $63°C$ correspond respectively to (100), (002), (101), (102), (110), and (103) peaks of hexagonal wurtzite polycrystalline ZnO structure (JCPDS card No. 00-036-1451).
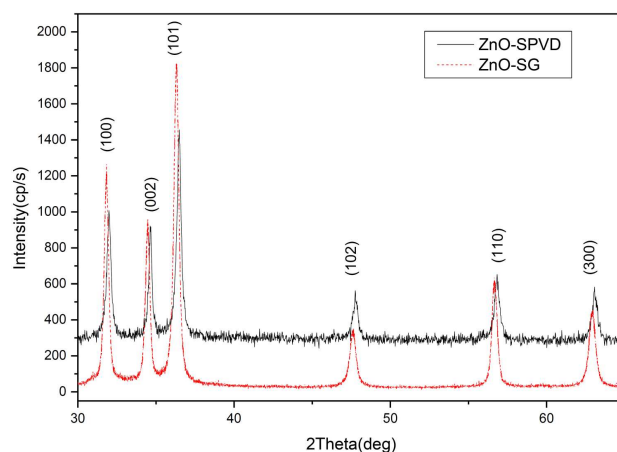

Fig. 2. XRD spectra of ZnO-SPVD and ZnO-SG catalysts.

Crystallite size was obtained by Debye-Scherrer formula given by equation [16,20]:

$$D = K\frac{\lambda}{\beta \ \cos\theta}, \tag{1}$$

where D is the crystallite size (in nm), 0.94 is the particle shape factor which depends on the shape of the particles (the typical value is 0.94), λ is the CuK_α radiations (1.5418 Å), β is full width at half maximum (FWHM) of the selected diffraction peak at angle $36°C$ corresponding to (101) plane and θ is the Bragg angle obtained from 2θ value corresponding to maximum intensity peak in XRD pattern. The mean crystallite size obtained using this formula was 36 nm for sol-gel derived particles and 26 nm in case of sublimation–condensation technique. In addition, the specific surface are calculated by the Gauss model was found to be 737.7 m^2g^{-1} and 759.3 m^2g^{-1} for ZnO-SPVD and ZnO-SG, respectively.

2.2.2. Raman spectra:

The Raman spectrum (RS) for the two catalysts samples was collected with a Bruker Senterra Dispersive Raman microscope spectrometer using 532 nm excitation from a 3B diode laser having $3cm^{-1}$ resolution

in the spectral region of 3700-45 cm^{-1}. The Raman spectra of ZnO nanoparticles prepared by sol-gel and sublimation–condensation methods are presented in Fig. 3.
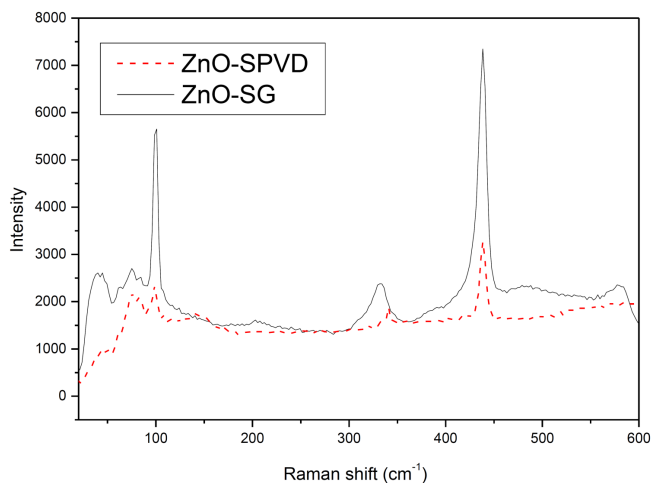

Fig. 3. Raman spectra of ZnO-SPVD and ZnO-SG catalysts.

The Raman spectrum for ZnO-SPVD was found to have peaks at (98 ± 1) cm^{-1}, (203 ± 1) cm^{-1}, (334 ± 1) cm^{-1}, (438 ± 1) cm^{-1}, and (570 ± 1) cm^{-1}. As for ZnO-SG, peaks at (99 ± 1) cm^{-1}, (203 ± 1) cm^{-1}, (334 ± 1) cm^{-1}, (390 ± 1) cm^{-1}, (438 ± 1) cm^{-1}, (483 ± 1) cm^{-1}, (577 ± 1) cm^{-1}, (581 ± 1) cm^{-1}, and (661 ± 1) cm^{-1} were observed. The peak at (438 ± 1) cm^{-1} in both samples was $E_{2(\text{high})}$ corresponding to the presence of crystalline wurtzite phase in ZnO. These results were consistent with the one obtained from XRD. Moreover, $E_{2(\text{high})}$ peak for ZnO-SG was more intense as compared to ZnO-SPVD. Since this mode is characteristic of ZnO Raman spectra and is associated with the motion of oxygen and zinc sublattices in the wurtzite structure of the oxide, as the intensity of this mode increases the degree of crystallinity of ZnO oxide heightens. That signifies less defects and good cristallinity in the ZnO-SG compared to ZnO-SPVD.

The vibration of the zinc sublattice $E_{2(\text{low})}$ is one of the most intense modes which peaked at about 98 cm^{-1}. The other weak peaks for both catalysts at 203 cm^{-1} were due to 2TA, $2E_{2(\text{low})}$, and at (334 ± 1) cm^{-1} were attributed to difference in frequency of $E_{2(\text{high})}$ and $E_{2(\text{low})}$. This was supposed to be originated from multiple-phonon scattering phenomenon [21].

These modes occur due to structural disorders in the host matrix. The peak at $(581 \pm 1$ cm$^{-1})$ in ZnO-SG was due to $A_{1\text{L}}$ mode. The result of Raman analysis provided the information regarding the improved crystallinity (greater crystallites) and structure (less of defects) of ZnO in ZnO-SG comparing with ZnO-SPVD.

2.3. Reactor and procedure

The experiments of the photocatalytic degradation were carried out in a glass reactor using an UV-A lamp (24 W) that emit at a region of wavelength between 320–400 nm and an emission peak at 365 nm. The light intensity of the radiation (60 W m^{-2}) was measured using a UV radiometer (VLX–3W equipped with a sensor CX-365). The experimental runs were carried out by using the following procedure for the dye: firstly 100 mL of the solution of the dye was taken into the reactor and a required amount of catalyst was added. Heterogeneous photodegradation and adsorption experiments were performed at room temperature $(25 \pm 1\,°\text{C})$ in a glass cell. The irradiated solutions and suspensions were magnetically stirred during whole experiments. The suspensions of dye and catalyst were stirred in the dark for 60 min before irradiation to establish adsorption/desorption equilibrium. The particles of ZnO were filtered after irradiation by Millipore filters of 0.2 μm.

2.4. Analyses

The amount of dye adsorbed onto the ZnO (mg g^{-1}) was calculated using the following relationship [14]:

$$Q_{\text{ads}} = \frac{(C_o - C_t)\,V}{m}, \tag{2}$$

where Q_{ads} is the adsorbed quantity at time t (mg g^{-1}), C_o is the initial dye concentration (mg L^{-1}), C_t is the dye concentration (mg L^{-1}) at the moment t of the process of adsorption, V is the volume of the solution (L), and m is the weight of adsorbent (g).

Degradation extent was calculated using the following equation:

$$\text{DEG removal}[\%] = \left[\frac{C_0 - C_t}{C_0}\right] \times 100 \tag{3}$$

where C_0 is the initial concentration of dye (mg L^{-1}) and C_t is the instant concentration of dye in the sample at time t (mg L^{-1}).

Pseudo-first-order reaction model has been widely and successfully used for the description of photocatalytic degradation of organic pollutants. The removal rates of dye in UV/ZnO (ZnO-SPVD and ZnO-SG) process is therefore expressed as [14]:

$$-\frac{\text{d}C_t}{\text{d}t} = \text{k}_{\text{app}} \times C_t \Leftrightarrow \ln\left(\frac{C_0}{C_t}\right) = \text{k}_{\text{app}} \times t, \tag{4}$$

where C_0 is the initial concentration of dye, C_t the concentration of dye at time t and k$_{\text{app}}$ (min^{-1}) is the pseudo-first-order photocatalytic removal rate constant.

3. Results and discussion

3.1. Adsorption study

It is likely that adsorption of the dye is an important parameter in determining photocatalytic degradation rate. Adsorption tests in dark were carried out in order to evaluate the equilibrium constants of the adsorption of the dye on the catalyst surface.

The most common model to describe adsorption process is the isotherm of Langmuir. The Langmuir adsorption isotherm is the most commonly used model to describe adsorption process. The linear transformation of Langmuir adsorption isotherm can be described by the following equations:

$$Q_e = \frac{Q_{max} K_L C_e}{1 + K_L C_e}, \tag{5a}$$

$$Q_e = \frac{Q_{max} K_L C_e}{1 + K_L C_e}, \tag{5b}$$

where C_e is the dye concentration at adsorption equilibrium, Q_e is the amount of dye adsorbed on the ZnO when equilibrium is achieved. Q_{max} is the theoretical maximum amount of dye adsorbed onto the ZnO surface, and K_L is the adsorption constant.

The linear transformation of Langmuir GV adsorption on the surface of each of ZnO-SG and ZnO-SPVD (Eq. (5)) are given in the Fig. 4. From the data obtained, the Langmuir adsorption equilibrium constants (Q_{max} and K_L) for both catalysts are given in Table I. Experimental results present a good correlation of the Langmuir model with correlation coefficients R^2 above 0.99 for both catalysts. This indicates unique adsorption sites, uniform monolayer adsorption, and no interaction between the adsorption sites. It appears that the adsorption coverage is small for both catalysts and the ZnO produced by the physical method (ZnO-SPVD) exhibits the higher adsorbed quantity. These results can be explained by the differences between the sizes of the two catalyst particles and surface areas. It has been found that the catalyst that has the smallest size of particles and larger surface area has the greatest adsorption capacity [14].
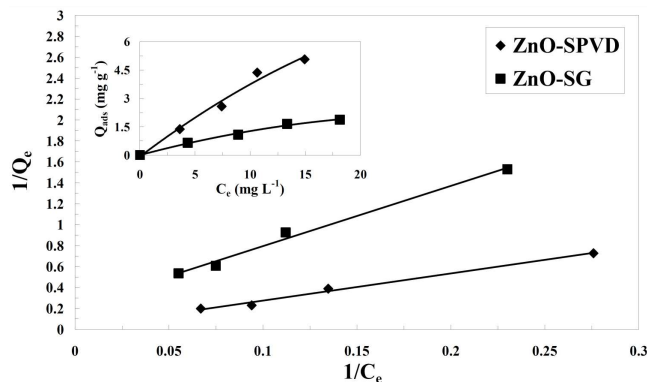

Fig. 4. Langmuir adsorption isotherm of GV on ZnO-SPVD and ZnO-SG: $Q_e = f(C_e)$. In the inset: transformation of Langmuir isotherm: $1/Q_e = f(1/C_e)$ ([Catalyst]=1 [g L^{-1}] and pH (5.7 ± 0.2)).

The adsorption isotherm $Q_e = f(C_e)$ for both catalysts are shown in the inset of Fig. 4. The evolution of Q_e as function of C_e for each of ZnO-SG and ZnO-SPVD catalysts, indicates that the Langmuir model is applicable for L-shape type [22]. L-shape type of

the isotherm means that there is no strong competition between the solvent and the adsorbate to occupy the adsorbent surface sites.

TABLE I

Langmuir adsorption equilibrium constants of GV on each of ZnO-SPVD and ZnO-SG.

	Q_{max} [mg g^{-1}]	K_L [L mg^{-1}]	R^2
ZnO-SPVD	71.43	0.0053	0.9914
ZnO-SG	4.58	0.0380	0.9905

3.2. Comparison of photocatalytic activity of ZnO-SPVD and ZnO-SG

In this study, the comparison between the activities of ZnO produced by SPVD and SG methods on the GV adsorption and photocatalytic degradation have been investigated at an amount of 1 g L^{-1} of catalyst and a concentration of 10 mg L^{-1} of GV at the natural solution pH of dye (pH 5.7 ± 0.2). The results of GV adsorption on the catalyst surface and GV degradation are shown in Fig. 5. As can be seen, the photodegradation reaction showed a significant degradation of GV for both catalysts. The degradation of GV reached 994% and 708% in 2 h during the photodegradation process for each of ZnO-SPVD and ZnO-SG, respectively.
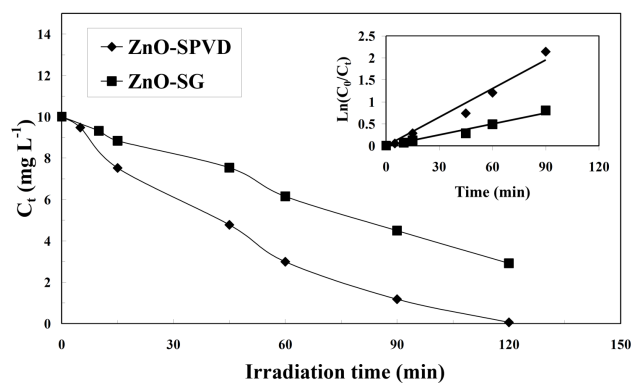

Fig. 5. Kinetics of GV disappearance by photocatalysis process with irradiation time in the presence of each of ZnO-SPVD and ZnO-SG. In the inset: Evaluation of pseudo-first order reaction kinetics ([GV]=10 [mg L^{-1}], [Catalyst]=1 [g L^{-1}] and pH (5.7 ± 0.2)).

Inset in the Fig. 5 shows that there is a good linear relationship between $\ln([GV_0]/[GV]_t)$ and irradiation time, which indicates that the GV degradation reaction follows the pseudo-first order kinetics with both catalysts. The values of rate constant of reaction were found to be 2.17×10^{-2} min^{-1} ($R^2 = 0.991$) and 8.3×10^{-3} min^{-1} ($R^2 = 0.992$) for ZnO-SPVD and ZnO-SG, respectively. It is shown that the rate constant of GV degradation in the presence of ZnO-SPVD is over 2.6 times higher than in the presence of ZnO-SG, indicating that the catalyst production method greatly affects its photocatalytic

efficiency. Also, the increase in the ZnO-SPVD efficiency can be attributed to its larger surface area compared to ZnO-SG; a large specific surface area and small crystal size will provide more active sites on the catalyst surface accelerating the production of $^\bullet$OH radicals that subsequently attack the dye molecules during the photocatalytic system.

3.3. Effect of initial dye concentration

The effect of initial dye concentration in water on the photocatalytic process has also been examined. The characteristic dyes concentrations in wastewater from textile industry are in the range from 5 to 30 mg L^{-1} [23]. Therefore, the reactions of the dye decomposition were carried out in this concentration range. The effect of various initial dyes concentrations on the GV photocatalytic decolorization has been investigated from 5 to 20 mg L^{-1}. The results are shown in Fig. 6.
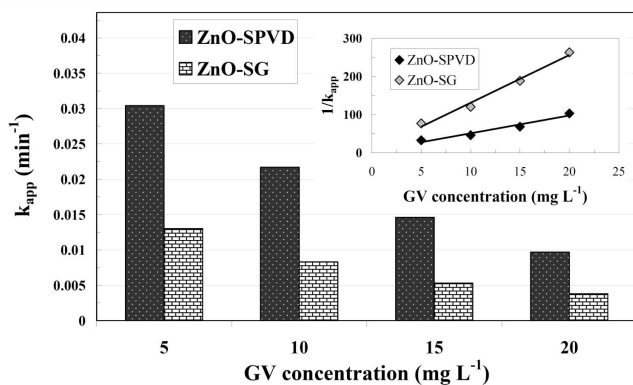

Fig. 6. Effect of initial GV concentration on the photocatalytic degradation. In the insert: transformation of Langmuir–Hinshelwood kinetic: $1/\mathrm{k_{app}} = f(C_e)$ ([Catalyst]=1 [g L^{-1}], pH (5.7 ± 0.2)).

As seen in in Fig. 6, degradation rate is inversely affected by the dye concentration. This negative effect can be explained by the fact that the increase in dye concentration also decreases the path length of photon entering into the dye solution. However, at high dye concentration a significant amount of UV-light may be absorbed by the dye molecules rather than the catalyst and this may also reduce the catalytic efficiency [24]. The decrease of apparent rate constant for high dyes concentrations can be also attributed to the decrease of active sites due to competition of photoproducts with substrate for the adsorption on the active sites of the ZnO surface [25] and the increase of degrading molecules towards the number of reactive species photogenerated ($^\bullet$OH, h^+).

The adsorption and photocatalytic degradation of model pollutants can be well described by the Langmuir–Hinshelwood (L–H) kinetic model:

$$r_0 = -\frac{\mathrm{d}C}{\mathrm{d}t} = \frac{k_r K_{L-H} C_e}{1 + K_{L-H} C_e} \qquad (6)$$

where r_0 (mg L^{-1} min^{-1}) is the initial rate of disappearance of the dye and C_e (mg L^{-1}) represent the amount of dye adsorbed onto the catalyst surface at equilibrium in the dark. K_{L-H} represents the equilibrium constant for adsorption of the dye onto ZnO and k_r reflects the limiting rate constant of reaction at maximum coverage under the given experimental conditions. This equation can be used when data demonstrate linearity plotted as follows:

$$\frac{1}{\mathrm{k_{app}}} = \frac{1}{k_r K_{L-H}} + \frac{C_e}{k_r} \qquad (7)$$

The applicability of L–H equation for the dye photodegradation has been confirmed by the linear plot obtained by plotting the $(1/\mathrm{k_{app}})$ against the (C_e) as shown in the inset in Fig. 6. The values of Langmuir–Hinshelwood equation constants of GV are listed in Table II. The adsorption equilibrium constant (K_{L-H}) obtained from this linearization is different to the constant obtained from the adsorption isotherm (K_L) and indicates that adsorption of the dye on the surface of ZnO particles plays a role in the photocatalytic reaction. The value of the adsorption constant K_{L-H} for photocatalytic degradation was about 200 times and 59 times higher than the adsorption constant K_L in the dark for ZnO-SPVD and ZnO-SG, respectively. There have been several studies reporting that K_{L-H} could be substantially larger than K_L [26, 27]. Various explanations have been suggested: (i) the improvement of the adsorption constant may be ascribed to the additional photoadsorption or the fast photocatalytic reaction under UV irradiation [28, 29]; (ii) UV-illumination would change electronic properties of the ZnO surface and thus the adsorptive sites [26, 30].

TABLE II

Langmuir–Hinshelwood constants of each of ZnO-SPVD and ZnO-SG

	K_r [mg L^{-1} min^{-1}]	K_{L-H} [L mg^{-1}]	R^2
ZnO-SPVD	0.215	1.06	0.960
ZnO-SG	0.445	2.25	0.987

3.4. Effect of pH

The most important parameter that influences the photocatalytic degradation of dyes is solution pH. Figure 7 presents the variation of the rate constant and the quantity of adsorbed GV as a function of solution pH for ZnO-SPVD and ZnO-SG catalysts.

The results show that photocatalytic degradation of the GV dye is strongly dependent on the pH of the solution. It was observed that the rate constant of GV degradation reaction increases with the increase of the solution pH for both catalysts.
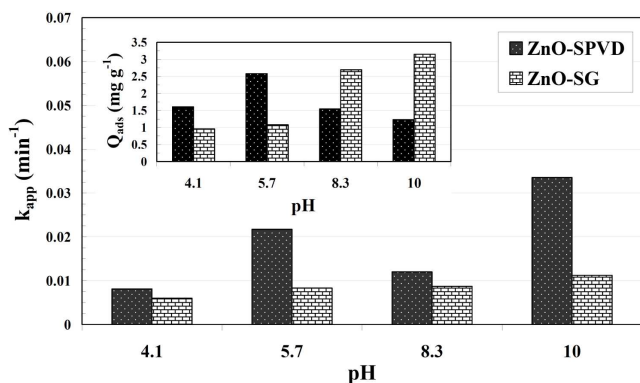
Fig. 7. Effect of pH on photocatalytic degradation of GV. In the inset: Effect of pH on the amounts of GV adsorbed on ZnO surface ([GV]=10 [mg L^{-1}] and [Catalyst]=1 [g L^{-1}]).

Fig. 8. Effect of H_2O_2 addition on the photocatalytic degradation of GV. In the inset: Effect of H2O2 addition on the amounts of GV adsorbed on ZnO surface ([GV]= 10 [mg L^{-1}], [Catalyst]=1 [g L^{-1}] and pH (5.7 ± 0.2)).

The photocatalytic removal of GV was observed to be fastest in alkaline pH for both catalysts and the ZnO-SPVD catalyst presents a higher degradation of GV at alkaline medium (pH 10) than the ZnO-SG catalyst. Since the GV adsorption is high at alkaline pH (inset in Fig. 7), the GV degradation is also efficient at these conditions. This reveals that the dye adsorption on catalyst surface plays a vital role in the dye degradation mechanism.

In addition, when the pH is slightly alkaline the rate constant of GV degradation increases due to availability of OH$^-$ ions in a concentration which is required for increasing the rate of reaction. These OH$^-$ ions generate $^\bullet$OH radicals which are effective in oxidizing species and responsible for the dye photocatalytic degradation.

3.5. Effect of H_2O_2 addition

The influence of H_2O_2 addition on the GV photocatalytic degradation reaction in the presence of ZnO-SPVD and ZnO-SG was investigated at an H_2O_2 concentration of 10^{-2} mol L^{-1}, and the results are shown in Fig. 8 for both catalysts. The amount of dye adsorbed on the catalyst surface in the absence or presence of H_2O_2 for both catalysts are shown in the inset in Fig. 8. The degradation rate increased with H_2O_2 addition for both catalysts with a ratio of 2.4 times and 6.5 times for ZnO-SPVD and ZnO-SG, respectively. It has been observed that the degradation of GV proceeds slightly faster in the presence of ZnO-SG as compared to ZnO-SPVD.

On the other hand, the adsorbed quantity of GV decreases after the addition of H_2O_2 for the two catalysts. In fact, the hydrogen peroxide molecules can compete with GV molecules on adsorption on the surface of the catalyst resulting in a decrease of GV adsorbed quantity on the surface of catalyst.

These results indicate that structural properties of the catalyst (average crystalline size and surface area) play an important role in the photocatalytic activity of the ZnO samples.
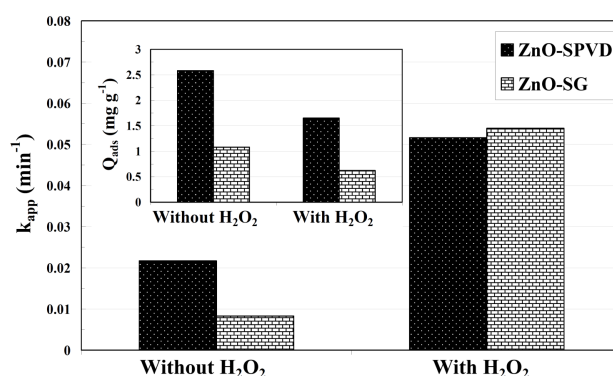
The enhancement of the dye degradation by the addition of H_2O_2 is due to the increase in the hydroxyl radical concentrations since it inhibits the $e^- \Leftrightarrow h^+$ recombination [14], according to equations:

$$H_2O_2 + e^- \rightarrow OH^- + {}^\bullet OH, \tag{8}$$

$$H_2O_2 + O_2^{\bullet -} \rightarrow {}^\bullet OH + OH^- + O_2. \tag{9}$$

3.6. Effect of HCO_3^- addition

The influence of NaHCO$_3$ (10^{-2} mol L^{-1}) at pH 8.3 (HCO$_3^-$ are the predominant species as pK$_a$ (HCO$_3^-$/CO$_3^{2-}$ = 10.2)) added to the GV degradation reaction has been studied, and the results are shown in Fig. 9. For both catalysts, the GVdegradation rate constant gradually increased with addition of increasing HCO$_3^-$ ions in the solution of GV with a ratio of 2.4 times and 1.6 times for ZnO-SPVD and ZnO-SG, respectively. It was observed that the degradation of GV proceed much more rapidly in the presence of ZnO-SPVD as compared to ZnO-SG. For adsorption results (inset in Fig. 9), the inhibition of the amount of adsorption of GV on the ZnO catalysts surface can be attributed to a competitive adsorption on the ZnO surface between these HCO$_3^-$ anions and the dye molecules.

The enhancement of GV degradation by addition of HCO$_3^-$ ions can be attributed on the fact that after the addition of HCO$_3^-$ ions the pH of solution increases to alkaline medium, pH of solution will be around 8.3. Thus, since GV is a cationic dye, it is positively charged in an alkaline medium, whereas, the ZnO surface will be negatively charged which leads to an electrostatic attraction between dye molecules and ZnO surface and adsorption could occur, and consequently, the GV degradation rate constant increases [31].

In addition, another reason can explain these results is that after the addition of HCO$_3^-$ ions, CO$_3^{\bullet -}$ radicals has been formed in the solution, since carbonate radicals can

attack the dye molecules and enhance the photocatalytic reaction, however, the $CO_3^{\bullet-}$ radicals are less reactive than $^{\bullet}OH$ radicals [16].
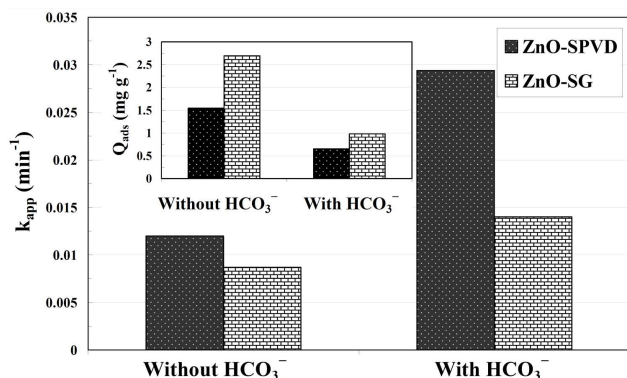

Fig. 9.   Effect of HCO_3^- addition on the photocatalytic degradation of GV. In the inset: Effect of HCO_3^- addition on the amounts of GV adsorbed on ZnO surface ([GV]= 10 [mg L^{-1}], [Catalyst]=1 [g L^{-1}] and pH 8.3).

4. Conclusion

The zinc oxide nano-structure was successfully synthesized by using sublimation–condensation technique (SPVD) and sol-gel method (SG) in nano-size range about 26 nm and 36 nm, respectively.

ZnO prepared using SPVD method was more efficient in the photocatalytic degradation of Gentian violet under UV radiation than the material prepared using SG method. These results indicate that the physical characteristics of the catalyst (particles size and specific surface area) play a vital role in the efficiency of the ZnO-based catalysts.

In an attempt to reach higher degradation efficiency of the GV dye solution, the effect of different operational parameters was studied. For both catalysts, the experimental results showed that the degradation rate increases with the decrease of the dye concentration; the degradation rate at alkaline medium was higher than that at natural and acidic one and the presence of H_2O_2 and HCO_3^- ions increased the effectiveness of the photodegradation. In the different conditions studied, a better photocatalytic activity of ZnO prepared by SPVD method (physical method) was observed compared to ZnO prepared by sol-gel method (chemical method). It was also observed by adsorption studies that the adsorption of dye is a prerequisite for the degradation process and there is a correlation between adsorption and photocatalytic degradation at different operator conditions.

Acknowledgments

References

[1] H.B. Zeng, W.P. Cai, P.S. Liu, X.X. Xu, H.J. Zhou, C. Klingshirn, H. Kalt, *Acs Nano* **2**, 1661 (2008).

[2] H. Zhang, J.B. Wu, C.X. Zhai, N. Du, X.Y. Ma, D. Yang, *Nanotechnol.* **18**, 455604 (2007).

[3] S. Bhatia, N.Verma·, *Mater. Res. Bull.* **95**, 468 (2017).

[4] B.O. Chin, Y.N. Law, M.A. Wahab, *Renew. Sust. Energ. Rev.* **81**, 536 (2018).

[5] D. Rajamanickam, M. Shanthi, *Arab. J. Chem.* **9**, S1858 (2016).

[6] J.R. Torres-Hernández, E. Ramírez-Morales, L. Rojas-Blanco, J. Pantoja Enriquez, G. Oskam, F. Paraguay-Delgado, B. Escobar-Morales, M. Acosta-Alejandro, L.L.Díaz-Flores, G. Pérez-Hernández, *Mater. Sci. Semicon. Proc.* **37**, 87 (2015).

[7] G.C. Hadjipanayis, R.W. Siegel, *Nanophase Materials: Synthesis–Properties–Applications*, Series E: Applied Science, KluwerAcademic Publishers, Dordrecht 1994, p. 260|.

[8] N. Lemée, C. Duboudieu, G. Delabouglise, J.P. Sénateur, F. Laroudie, *J. Cryst. Growth* **235**, 347 (2002).

[9] K.P. Surendran, A. Wu, P.M. Vilarinho, V.M. Ferreira, *Chem. Mater.* **20**, 4260 (2008).

[10] F. Maxim, P. Ferreira, P.M. Vilarinho, I. Reaney, *Cryst. Growth Design* **8**, 3309 (2008).

[11] K.V. Saravanan, M.G. Krishna, K.C.J. Raju, A.K. Bhatnagar, *J. Mater. Sci.* **42**, 1149 (2007).

[12] E. Neyens, J. Baeyens, *J. Hazar. Mater.* **98**, 33 (2003).

[13] S. Parsons, *Advanced Oxidation Processes for Water and Wastewater Treatment*, IWA Publishing, Cornwall (UK) 2004.

[14] N. Bouanimba, R. Zouaghi, N. Laid, T. Sehili, *Desalination* **275**, 224 (2011).

[15] H.S. Rai, M.S. Bhattacharya, J. Singh, T.K. Bansal, P. Vats, U.C. Banerjee., *Crit. Rev. Env. Sci. Technol.* **35**, 219 (2005).

[16] N. Bouanimba, N. Laid, R. Zouaghi, T. Sehili, *Int. J. Chem. React. Eng.* , 20170014 (2017).

[17] Y. Liu, J. Lin, M. Chen, L. Song, *Food and Chem. Toxicol.* **58**, 264 (2013).

[18] H. Benhebal, M. Chaib, M. Crine, A. Léonard, S. Lambert, *Chiang Mai J. Sci.* **42**, 585 (2016).

[19] A. Rouanet, H. Solmon, G. Pichelin, C. Roucau, F. Sibieude, C. Monty, *Nanostruct. Mater.* **6**, 283 (1995).

[20] T.L. Thompson, J.T. Yates. S, *Chem. Rev.* **106**, 4428 (2006).

[21] D. Das, P. Mondal, *RSC Adv.* **4**, 35735 (2014).

[22] C.H. Giles, A.P. D'Silva, I.A. Easton, *J. Colloid Interface Sci.* **47**, 766 (1974).

[23] M. Vautier, C. Guillard, J.M. Herrmann, *J. Catal* **201**, 46 (2001).

[24] A. Mills, R.H Davis, D. Worsley, *Chem Soc Rev* **22**, 417 (1993).

[25] N. Serpone, E. Pelizzetti, *Photocatalysis: Fundamentals and Application*, Wiley Interscience, New York 1989.

[26] E. Vulliet, J.M. Chevelon, C. Guillard, J.M. Hermann, *Photochem. Photobiol* **159**, 71 (2003).

[27] J. Cunningham, G. Al-Sayyed, S. Srijaranai, *Adsorption of Model Pollutants onto TiO_2 Particles in Relation to Photoremediation of Contamined Water* in: *Aquatic and Surface Photochemistry*, Ch. 22, Eds. G. Helz, R.D. Zepp, D. Crosby, Lewis Publs, CRC Press, Boca Raton (FL) 1994, p. 317.

[28] S. Qourzal, M. Tamimi, A. Assabbane, Y. Ait-Ichou, *Colloid. Interf. Sci.***286**, 621 (2005).

[29] Y. Meng, X. Huang, Y. Wu, X. Wang, Y. Qian, *Environ. Pollut* **117**, 307 (2002).

[30] M. Sleiman, D. Vildozo, C. Ferronato, J.M. Chovelon, *Appl. Catal. B: Environ* **77**, 1 (2007).

[31] N. Laid, N. Bouanimba, R. Zouaghi, T. Sehili, *Desalin. Water Treat.* **57**, 1935 (2016).